

RESEARCH PAPER

Automated extraction of device noise parameters based on multi-frequency, source-pull data

SERGIO COLANGELI, WALTER CICCOGNANI, MIRKO PALOMBA AND ERNESTO LIMITI

In this paper a novel approach for determining the four noise parameters of FET devices over frequency is presented. Such methodology is made of two parts: the first one allows to straightforwardly extract single-frequency noise parameters from source-pull data; the second one extends this capability to multi-frequency, source-pull data to obtain a full description of device noise behavior over frequency by means of at most 10 constant parameters (depending on the required accuracy). The whole process is automated via a software routine and does not need a previous knowledge of the FET equivalent circuit's topology, or the values of its elements. This peculiarity makes the proposed method very well suited to quick characterization campaigns of active devices, avoiding the burden of a whole set of prior, different measurements and the relevant, critical extraction procedures, which are strongly dependent on the device.

Keywords: Modeling, Simulation and characterizations of devices and circuits, Microwave measurements

Received 26 October 2012; Revised 16 July 2013; first published online 10 September 2013

I. INTRODUCTION

It is well known that the overall sensitivity of almost any receiving chain is largely determined by the noise and gain performance of the first amplifying stage. For this reason a great effort is being spent by foundries and research groups, aiming at optimizing technological processes and seeking novel, sophisticated design methodologies [1]. On the other hand, for low-noise designs to be reliable, an accurate determination of active device noise parameters is a key step, therefore many approaches can be found in the open literature to extract the noise parameters of FETs.

Several works [2–5] describe the noise behavior of the active channel through a small-signal equivalent circuit and frequency-independent parameters. In particular, Pospieszalski [4] (also verified by Tasker [5]) models the noise of the active channel utilizing thermal equivalent noise sources, assigned to the equivalent circuit resistors: such approach leads to the extraction of two (or one) unknown equivalent temperatures based on noise figure measurements of the device (typically input terminated on the Noise Source) over a broad frequency range. An accurate knowledge of all the equivalent circuit elements is however needed. Dambrine [6] proposes an extraction procedure making use of an extrinsic device and two frequency-independent external equivalent noise temperatures to reduce the number of the

parasitic elements required for the determination of the FET noise parameters to three (instead of – at least – eight). De Dominicis [7] proposes a method utilizing the Y -parameters of the device and two frequency-independent equivalent noise temperatures, not requiring therefore any information concerning the equivalent circuit of the device, resulting in a model that is effective in the frequency range where the electrical effects of the parasitic elements are negligible. Serino [8] obtains the noise model of the FET by using the small signal H -parameters of the device and defining two frequency-dependent equivalent noise temperatures (three constant parameters to be determined): also this approach only requires S -parameters and F_{50} measurements only but its validity holds up to 80% of the device f_{max} .

As can be noted, the target application of the above methods is to noise data where the DUT input termination is fixed, or in any case cannot be arbitrarily tuned. When such a possibility does exist – as is the case of automated noise test benches such as that proposed by the authors in a previous work [9] – a Source-Pull-based extraction method can be adopted. In the latter case, the characterization is obviously not restricted to active devices only. Following the algorithm proposed by Lane [10], a mathematical transformation can be performed from the usual noise parameters (F_{min} , R_n , and Γ_{opt}) to four fictitious parameters (A , B , C and D), which allows to express the noise factor as a linear function of such new unknowns and, eventually, to solve for them via a simple matrix inversion (or pseudo-inversion, in case of an over-dimensional system). This method must be applied at each frequency by measuring the noise factor for at least four different input terminations.

Department of Electronic Engineering, University of Roma “Tor Vergata”, Via del Politecnico, 1, Roma, 00133, Italy

Corresponding author:

S. Colangeli

Email: colangeli@ing.uniroma2.it

In this work a novel extraction technique is presented which is featured by the following peculiarities: first, it can be shown to be mathematically equivalent, at single frequency, to Lane’s algorithm and, second, it can be easily extended in order to be applied to multi-frequency, Source-Pull noise data. This technique assumes a polynomial model for the FET’s noise correlation terms, which can be verified to be valid for a broad frequency range and for a variety of different devices, irrespective of the peculiarities of their equivalent circuit: in fact, the equivalent circuit’s topology and elements do not even need to be known.

The single-frequency extraction method is discussed in Section II, while the polynomial model and the multi-frequency technique are the subject of Section III. Finally, in Section IV a real example of noise extraction is reported and discussed.

II. ITERATED SINGLE-FREQUENCY EXTRACTIONS

In established theory of linear noisy networks (see for instance [11]), two-ports can be represented at a given frequency as in Fig. 1(a), where [S] is the two-port scattering matrix and [C] is its noise correlation matrix. It can be shown that the noise properties of the two-port can be de-embedded so as to obtain an equivalent representation, as in Fig. 1(b). The relationship between the noise sources e_n and i_n in Fig. 1(b) and the correlation matrix (here considered in “ABCD” form) is as follows:

$$C = \begin{bmatrix} c_{11} & c_{12} \\ c_{21} & c_{22} \end{bmatrix} = \begin{bmatrix} c_{11} & c_{12} \\ c_{12}^* & c_{22} \end{bmatrix} = \begin{bmatrix} \overline{e_n e_n^*} & \overline{e_n i_n^*} \\ \overline{e_n^* i_n} & \overline{i_n i_n^*} \end{bmatrix} \quad (1)$$

where the bar indicates the mean value and the star indicates the complex conjugate. Furthermore, the correlation parameters can be linked to classic noise parameters by the following equations:

$$\begin{cases} R_n = \frac{c_{11}}{4k_B B T_o} = \hat{c}_{11} \\ Y_\gamma = \frac{c_{12}^*}{c_{11}} = \frac{\hat{c}_{12}^*}{\hat{c}_{11}} \\ G_u = \frac{c_{22} - c_{11} \cdot |Y_\gamma|^2}{4k_B B T_o} = \hat{c}_{22} - \hat{c}_{11} \cdot |Y_\gamma|^2 \end{cases} \quad (2)$$

where the cap represents the normalization on $4k_B B T_o$, k_B being Boltzmann’s constant, B the bandwidth and $T_o = 290$ K the standard noise temperature. By means of these parameters, the two-port noise factor can be expressed as a function of the source admittance $Y_S = G_S + jB_S$:

$$F(Y_S) = 1 + \frac{G_u + R_n \cdot |Y_S - Y_\gamma|^2}{G_S} \quad (3)$$

Note that all representations of the two-port noise properties are equivalent and account for four real parameters (two real numbers and a complex one in the case of (1) and of (2)). The “Source-Pull” technique applied to noise characterization allows extracting such parameters at a given frequency by means of at least four measurements of noise factor, each on a different input termination. In order to avoid an ill-

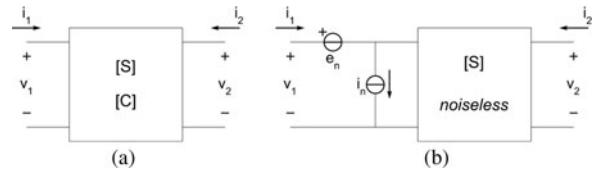


Fig. 1. Representations of a linear, noisy two-port (a) and its equivalent circuit with external noise sources (b).

conditioned system of equations and to reduce extraction uncertainties, a much higher number of measurements are usually taken in practice, and a least-squares minimization is then performed on an over-dimensioned system.

However, a direct application of a least-squares algorithm on a nonlinear function of the unknowns, as is (3), may result in multiple and/or unphysical solutions, unless a good initial guess is provided. Various solutions have been proposed to this problem (see for instance [12]), but the most used is that introduced by Lane [10]: his work starts from an alternative expression of F as a nonlinear function of F_{min} , R_n , and Y_{opt} :

$$F(Y_S) = F_{min} + \frac{R_n}{G_S} |Y_S - Y_{opt}|^2 \quad (4)$$

where:

$$\begin{cases} R_n = \hat{c}_{11} \\ Y_{opt} = G_{opt} + jB_{opt} = \frac{\sqrt{\hat{c}_{11}\hat{c}_{22} - \Im\{\hat{c}_{12}\}^2}}{\hat{c}_{11}} + j\frac{\Im\{\hat{c}_{12}\}}{\hat{c}_{11}} \\ F_{min} = 1 + 2\Re\{\hat{c}_{12}\} + 2\sqrt{\hat{c}_{11}\hat{c}_{22} - \Im\{\hat{c}_{12}\}^2} \\ \quad = 1 + 2\Re\{\hat{c}_{12}\} + 2R_n G_{opt} \end{cases} \quad (5)$$

which is then transformed into a linear function of four new, factitious unknowns A , B , C and D :

$$F(Y_S) = A + B \cdot \left(G_S + \frac{B_S^2}{G_S} \right) + C \cdot \frac{1}{G_S} + D \cdot \frac{B_S}{G_S} \quad (6)$$

These parameters, which must not be confused with the terms of the transmission (ABCD) matrix, are related to the conventional noise parameters through the following relationships:

$$\begin{cases} F_{min} = A + \sqrt{4BC - D^2} \\ R_n = B \\ G_{opt} = \Re\{Y_{opt}\} = \frac{\sqrt{4BC - D^2}}{2B} \\ B_{opt} = \Im\{Y_{opt}\} = \frac{-D}{2B} \end{cases} \quad (7)$$

Since $F(Y_S)$ is linear with respect to A , B , C and D , a least-squares algorithm can now easily be implemented, possibly after defining a suitable error function, W_i . Indeed, by explicitly computing and then setting to zero the partial derivatives of the error function with respect to the four unknowns, it is possible to build a non-singular linear system of equations [10].

Alternatively, we propose to take advantage of the sophisticated, built-in capabilities of modern computation environments (such as MATLAB®) and simply solve for the four

unknowns by pseudo-inverting an over-determined linear system, which can be expressed in matrix form as follows:

$$\begin{bmatrix} F(Y_{S,1}) \\ F(Y_{S,2}) \\ \vdots \\ F(Y_{S,n}) \end{bmatrix} = \begin{bmatrix} 1 & G_{S,1} + \frac{B_{S,1}^2}{G_{S,1}} & \frac{1}{G_{S,1}} & \frac{B_{S,1}}{G_{S,1}} \\ 1 & G_{S,2} + \frac{B_{S,2}^2}{G_{S,2}} & \frac{1}{G_{S,2}} & \frac{B_{S,2}}{G_{S,2}} \\ \vdots & \vdots & \vdots & \vdots \\ 1 & G_{S,n} + \frac{B_{S,n}^2}{G_{S,n}} & \frac{1}{G_{S,n}} & \frac{B_{S,n}}{G_{S,n}} \end{bmatrix} \cdot \begin{bmatrix} A \\ B \\ C \\ D \end{bmatrix} \quad (8)$$

where measurements are numbered from 1 to n . The number of measurements, n , should be adequate to the uncertainty estimated for the particular setup and in no case can be less than 4: for an analysis of the role of the number and pattern of measurement source impedances on the final accuracy, refer for instance to [13].

In the present work we will show that an approach similar to Lane’s can be adopted, which relies only on classic, physical parameters, i.e. the correlation matrix elements. To demonstrate this, it is sufficient to substitute (2) in (3), which yields:

$$\begin{aligned} F(Y_S) &= 1 + \frac{G_u + R_n \cdot |Y_S - Y_\gamma|^2}{G_S} \\ &= 1 + \frac{\hat{c}_{22} - \hat{c}_{11} \cdot |Y_\gamma|^2 + \hat{c}_{11} \cdot |Y_S - Y_\gamma|^2}{G_S} \\ &= 1 + \frac{\hat{c}_{22} - \hat{c}_{11} \cdot |Y_\gamma|^2 + \hat{c}_{11} \cdot (|Y_S|^2 + 2\Re\{Y_S \cdot Y_\gamma^*\} + |Y_\gamma|^2)}{G_S} \\ &= 1 + \frac{\hat{c}_{22} + \hat{c}_{11} \cdot |Y_S|^2 + 2\Re\{Y_S \cdot \hat{c}_{12}\}}{G_S} \end{aligned} \quad (9)$$

This equation can be rearranged so as to leave in the right-hand member only the four unknowns with their coefficients:

$$(F(Y_S) - 1) \cdot G_S = |Y_S|^2 \cdot \hat{c}_{11} + 2G_S \cdot \Re\{\hat{c}_{12}\} - 2B_S \cdot \Im\{\hat{c}_{12}\} + \hat{c}_{22} \quad (10)$$

where the left-hand side is clearly linear with respect to \hat{c}_{11} , $\Re\{\hat{c}_{12}\}$, $\Im\{\hat{c}_{12}\}$ and \hat{c}_{22} . Therefore, also in this case we can readily set up an over-dimensioned system of linear equations in matrix form:

$$\begin{bmatrix} (F(Y_{S,1}) - 1) \cdot G_{S,1} \\ (F(Y_{S,2}) - 1) \cdot G_{S,2} \\ \vdots \\ (F(Y_{S,n}) - 1) \cdot G_{S,n} \end{bmatrix} = \begin{bmatrix} |Y_{S,1}|^2 & 2G_{S,1} & -2B_{S,1} & 1 \\ |Y_{S,2}|^2 & 2G_{S,2} & -2B_{S,2} & 1 \\ \vdots & \vdots & \vdots & \vdots \\ |Y_{S,n}|^2 & 2G_{S,n} & -2B_{S,n} & 1 \end{bmatrix} \cdot \begin{bmatrix} \hat{c}_{11} \\ \Re\{\hat{c}_{12}\} \\ \Im\{\hat{c}_{12}\} \\ \hat{c}_{22} \end{bmatrix} \quad (11)$$

and immediately solve for \hat{c}_{11} , $\Re\{\hat{c}_{12}\}$, $\Im\{\hat{c}_{12}\}$ and \hat{c}_{22} by means of a pseudo-inversion.

It can be shown that (10) is equivalent to (6). To this end, an expression of Lane’s parameters in terms of standard noise

parameters must previously be derived:

$$\begin{cases} A = 1 + 2R_n G_\gamma \\ B = R_n \\ C = G_u + |Y_\gamma|^2 R_n \\ D = 2R_n B_\gamma \end{cases} \quad (12)$$

Hence substituting (12) in (6) leads after some math to:

$$(F(Y_S) - 1) \cdot G_S = R_n |Y_S|^2 + 2R_n G_\gamma G_S + 2R_n B_\gamma B_S + R_n |Y_\gamma|^2 + G_u \quad (13)$$

which exactly matches (10) since the following identities hold:

$$\begin{cases} R_n = \hat{c}_{11} \\ R_n G_\gamma = \Re\{\hat{c}_{12}\} \\ R_n B_\gamma = \Im\{\hat{c}_{12}\} \\ R_n |Y_\gamma|^2 + G_u = \hat{c}_{22} \end{cases} \quad (14)$$

However, it should be stressed, the mathematical equivalence between (10) and (6) does not guarantee that Lane’s algorithm and the proposed one give the same results when applied to real-world data, which indeed are affected by measurement errors: in this case the two methods may not fully agree – sometimes one or both may even yield unphysical results. For this reason, it is advisable to apply both methods to the data collected in measurement campaigns, in the best case to validate one with the other, otherwise to try and get at least one set of physical parameters.

With regard to the issue of measurement errors, it was mentioned earlier that a straightforward way of minimizing their effect is to take a number of measurements greater than the number of unknowns, that is $n > 4$. Another good practice, when applicable, consists in weighting each row of the linear system, based on the reliability of the relevant measurement: of course, the evaluation of a weighting function, W_i , depends on specific factors and can not always be determined. However, when a proper knowledge of the measuring set-up is available and W_i can be devised, it can be taken into account as a multiplicative factor of each i -th system row in (8) or (11). Ideally, if the negative effects of poorly accurate measurements are efficiently reduced by weighting, any extraction method such as Lane’s or the proposed one is expected to lead to similar results.

III. MULTI-FREQUENCY EXTRACTION

It is empirically found that, for a typical high-frequency active device, the four terms of the correlation matrix can be easily fitted by Taylor polynomials of (at most) the third degree, over a frequency band at least up to f_{max} (provided non-white noise generation mechanisms are neglected):

$$\begin{aligned} \hat{c}_{11} &= +\alpha_0 + \alpha_1 f + \alpha_2 f^2 + \alpha_3 f^3 \\ \Re\{\hat{c}_{12}\} &= +\beta_0 + \beta_1 f + \beta_2 f^2 + \beta_3 f^3 \\ \Im\{\hat{c}_{12}\} &= +\gamma_0 + \gamma_1 f + \gamma_2 f^2 + \gamma_3 f^3 \\ \hat{c}_{22} &= +\delta_0 + \delta_1 f + \delta_2 f^2 + \delta_3 f^3 \end{aligned} \quad (15)$$

where f is the frequency. As an example, in Fig. 2 the

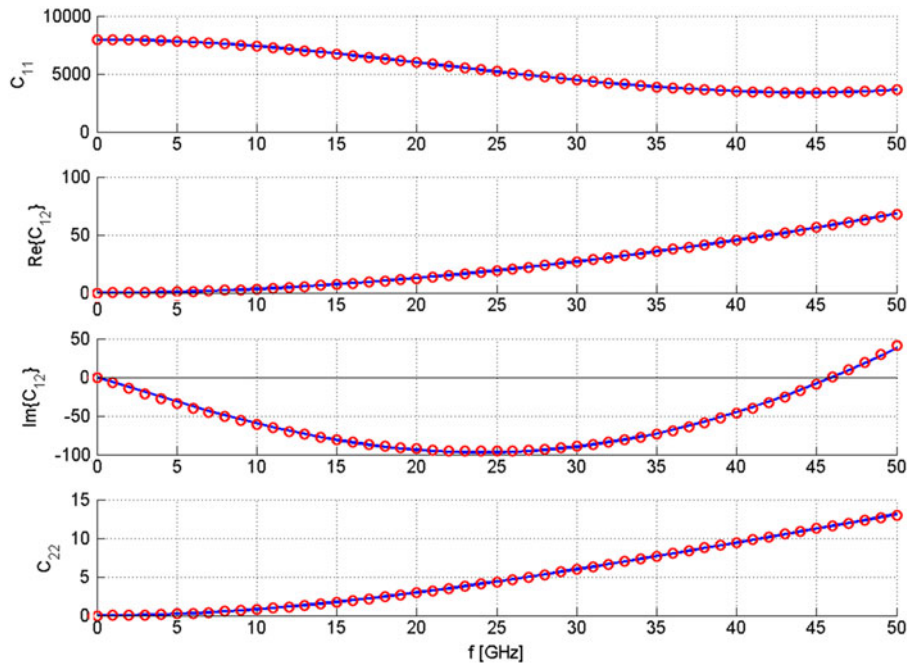


Fig. 2. Elements of the noise correlation matrix of a GaN HEMT over frequency.

correlation matrix of an ideal FET (whose parameters are based on equivalent circuit extractions [14]) are plotted: the computed behavior (continuous trace) is excellently fitted by third-degree polynomials (circle markers) well beyond f_{max} which equals 58 GHz for the considered FET device. Rather than to f_{max} , however, it is sounder to relate the range of validity of this polynomial fitting to f_n , which denotes in this work the positive frequency at which the optimum source termination, Y_{opt} , crosses the real axis. From (5), we see that f_n can be found as the frequency at which $\Re\{\hat{c}_{12}\}$, which is zero for $f = 0$ and negative for low frequencies, becomes zero again.

Since the parameters of the correlation matrix could be explicitly computed as functions of the device’s small-signal equivalent circuit and of its frequency-independent noise temperatures [8], one may try and exploit such closed-form expressions to show that, typically, not all 16 Taylor coefficients are significant. However, this approach would imply unmanageable formulae, requiring sophisticated symbolic math programs to be successfully undertaken.

Instead of relying on such tools, we will demonstrate how the same results can be attained starting from the following low-frequency relationships, which should be quite familiar to the reader (anyway, they can be easily verified empirically for a typical FET):

$$F_{min}|_{f \approx 0} \simeq 1 + k_{F_{min}} f \quad , \quad k_{F_{min}} > 0 \quad (16)$$

$$G_{opt}|_{f \approx 0} \simeq k_{G_{opt}} f \quad , \quad k_{G_{opt}} = \frac{F_{min} - 1}{2R_n} > 0 \quad (17)$$

$$B_{opt}|_{f=0} \simeq k_{B_{opt}} f \quad , \quad k_{B_{opt}} < 0 \quad (18)$$

$$R_n|_{f \approx 0} \simeq R_{n,o} \quad (19)$$

In particular, using (16)–(19) together at $f = 0$ yields:

$$\Re\{\hat{c}_{12}\}|_{f=0} = \Im\{\hat{c}_{12}\}|_{f=0} = \hat{c}_{22}|_{f=0} = 0, \quad \hat{c}_{11}|_{f=0} = R_{n,o} > 0 \quad (20)$$

Equations (19) and (20) allow us to null β_o , γ_o , δ_o and α_1 in (15).

Analogously, comparing (17) to (5) for small frequencies implies that $\Re\{\hat{c}_{12}\}$ and its derivative are zero when computed at $f = 0$, therefore β_1 also should be set to zero. On the contrary, γ_1 cannot be zeroed, since from (5) and (18) it is found to be strictly negative for typical devices: this is also confirmed by studying the low-frequency behavior of the noise factor on a constant termination, which from (9) is linear with slope $-2\gamma_1(B_S/G_S)$. As to γ_2 , this coefficient is expected from (5) to be positive if we simplify the model by neglecting γ_3 : this relates to the fact that B_{opt} approaches zero after a range of frequencies over which it is negative.

Finally, if we express G_{opt} as a function of the coefficients α_o , $\alpha_1 \dots \delta_3$ and neglect, inside the radix, the terms with a degree higher than 2, we obtain

$$\begin{aligned} G_{opt}|_{f \approx 0} &\simeq \frac{1}{\alpha_o} \sqrt{\alpha_o \delta_1 f + (\alpha_o \delta_2 - \gamma_1^2) f^2} \\ &= \frac{\sqrt{\alpha_o \delta_2 - \gamma_1^2}}{\alpha_o} f \end{aligned} \quad (21)$$

where δ_1 is zeroed to preserve the validity of (17).

As a by-product of equation (21), we get that $\delta_2 > 0$, since α_o and γ_1^2 are obviously positive. The condition $\alpha_o > 0$, together with $\alpha_2 < 0$ and $\alpha_3 > 0$, is the immediate consequence of the behavior versus frequency of $\hat{c}_{11} > 0$ – more precisely, by exploiting the fact that $\alpha_1 = 0$, we can derive the following relationship among the coefficients α_i :

$\frac{|\alpha_2|}{\alpha_3} < \sqrt[3]{\frac{\alpha_0}{(2\alpha_3)^2}} + \sqrt[3]{\frac{2\alpha_0}{\alpha_3}}$. Furthermore, since $\hat{c}_{22} > 0$ and

$\delta_0 = \delta_1 = 0$, we can also state that $\delta_2 > 0$, $\delta_3 \geq -\frac{\delta_3}{f_n}$, where we are assuming that the model is valid at least up to f_n .

All the previous inequalities can be used to test the meaningfulness of an extraction (it would be difficult to embed them in the extraction itself). As to the terms that we showed to be null, on the other hand, we can cancel them out from (15), thus obtaining the following 10-coefficient model:

$$\begin{aligned} \hat{c}_{11} &= +\alpha_0 && +\alpha_2 f^2 && +\alpha_3 f^3 \\ \Re\{\hat{c}_{12}\} &= && +\beta_2 f^2 && +\beta_3 f^3 \\ \Im\{\hat{c}_{12}\} &= && +\gamma_1 f && +\gamma_2 f^2 && +\gamma_3 f^3 \\ \hat{c}_{22} &= && +\delta_2 f^2 && +\delta_3 f^3 \end{aligned} \quad (22)$$

where terms $\beta_3 f^3$, $\gamma_3 f^3$ and $\delta_3 f^3$ allow to refine the fitting, but could be neglected in many cases. Furthermore, in some practical cases (see Section IV) other simplifications are possible.

It is worthwhile noting that the polynomial representations introduced in this Section are particularly well suited to well-behaving active devices, but cannot be used to model any generic two-port. The most clear case demonstrating this, is that of a chain of a transmission line (or any distributed network) and a FET: the line will introduce periodic effects in the overall noise resistance and optimum noise match, thus preventing one from exploiting model (15) and its simplified versions.

Two possibilities now arise as far as the determination of such coefficients is concerned:

- (a) treating each of them as a fitting parameter of the relevant \hat{c}_{ij} term;
- (b) substituting (22) in (11), so as to obtain a new system of the same form but in the unknowns $\alpha_0, \alpha_2 \dots \delta_3$. The vector of constants will remain unchanged, while the characteristic matrix rows and the vector of unknowns will grow in dimension. The i -th equation will appear as follows:

$$\begin{aligned} (F(Y_{S,i}) - 1) \cdot G_{S,i} = & \\ \left[\begin{array}{c} |Y_{S,i}|^2 \cdot \begin{bmatrix} 1 \\ f^2 \\ f^3 \end{bmatrix}^T \\ 2G_{S,i} \cdot \begin{bmatrix} f^2 \\ f^3 \end{bmatrix}^T \\ -2B_{S,i} \cdot \begin{bmatrix} f \\ f^2 \\ f^3 \end{bmatrix}^T \end{array} \right] \cdot \begin{bmatrix} \alpha_0 \\ \alpha_2 \\ \alpha_3 \\ \beta_2 \\ \beta_3 \\ \gamma_1 \\ \gamma_2 \\ \gamma_3 \\ \delta_2 \\ \delta_3 \end{bmatrix} \end{aligned} \quad (23)$$

Notice that a model as simple as that in (22) would be difficult to justify if one attempted a direct approximation of Lane’s parameters, since their relationships to classic noise parameters are less familiar than those of the correlation matrix terms. Therefore, although it is maybe feasible to extend approach (b) directly to Lane’s parameters, this would require a specific work, which was not addressed by the authors. However, one may use Lane’s algorithm to determine the classical noise parameters, then compute the \hat{c}_{ij} terms and finally apply approach (a).

Method (a) is based on a previous extraction of each \hat{c}_{ij} term versus measurement frequencies by repeatedly applying (11): as a consequence, the determination of the correlation matrix is independent for every frequency, and the subsequent fitting process is independent for each \hat{c}_{ij} term. On the contrary, approach (b) is expected to be somewhat more robust since all unknowns are computed through one single-step extraction: in other words, measurements at a given frequency influence the resulting model at every frequency, thus contributing to under-weight possible outliers. However, both methods are feasible and typically lead to good results even when applied to measurements affected by random errors.

A thoroughly analysis of the robustness of the proposed methodologies to measurement errors is beyond the scope of this work. Not only would such an analysis be very complex, due to the inherent complexity of the algorithms under consideration, but it would also depend on a large number of parameters, such as the frequency sweep used, the source pattern, the DUT’s behavior, the errors made in characterizing the blocks along the measurement and calibration paths, the errors in noise readings. Besides the difficulties related to managing this mass of input quantities in a comprehensive, meaningful way, the risk arises of losing the focus on the proposed methodologies and centering the attention, instead, on the features of the particular setup.

Therefore, only a simplified case will be discussed, based on simulated data, to give the reader a feel of the numbers involved. In particular, all sources of error will be merged so that a single, random value, with zero mean and uniformly distributed in an interval of width ΔNF [dB], can be added to each noise figure measurement – irrespective of frequency and source state. This choice allows, at least approximately, to disregard the characteristics of the specific test bench. Moreover, a frequency sweep from 5.1 to 20.1 GHz, step 1 GHz, will be assumed to fix ideas, as well as a 30-point pattern of source reflection coefficients, with magnitudes of 0.2, 0.4 and 0.6, and angles spaced of 36° .

The left side of Fig. 3 shows a typical example of noise parameters extraction following the single-frequency method and approaches (a) and (b) – denoted by round, “times” and triangle markers, respectively – for different values of ΔNF , from 0 to 1 dB. It is readily noted that single-frequency extractions exhibit an irregular behavior also for low values of ΔNF , as opposed to multi-frequency approaches, which accurately replicate the true parameters for values of ΔNF below 0.75 dB. In particular, approach (b) yields accurate values of all noise parameters also for low frequencies, outside the measurement bandwidth, while approach (a) is not as correct on noise resistance.

A more quantitative comparison is reported on the right side of Fig. 3, which shows maximum percent errors of the extracted parameters (computed as $(x_{meas}/x_{true} - 1) \times 100$ for the generic parameter x) versus ΔNF in the measurement

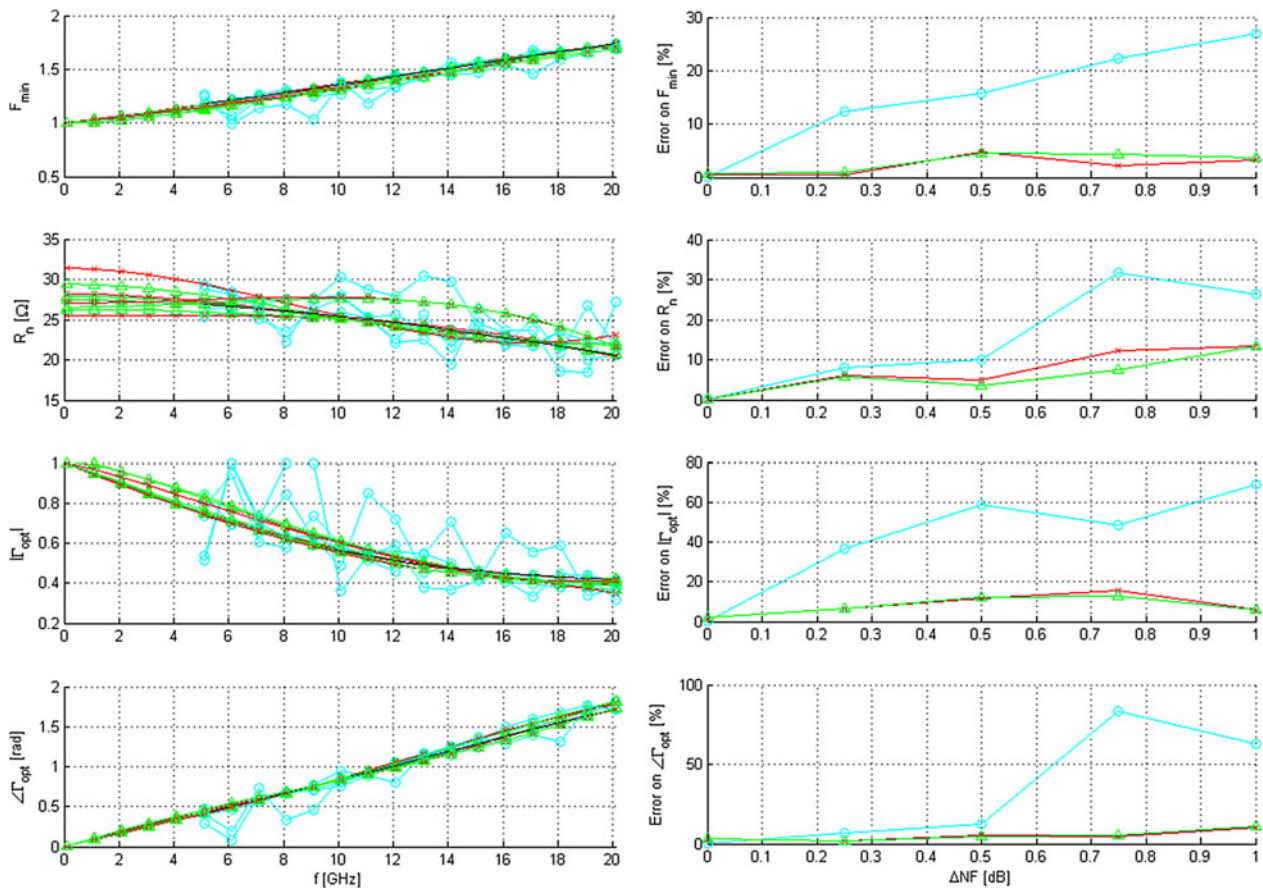


Fig. 3. Effect of measurement errors on noise parameter extraction for an ideal HEMT, with a 30-state pattern. Left side: example of extraction using the proposed methodologies for zero-mean measurement errors uniformly distributed in a range ΔNF [dB]. Right side: maximum percent errors versus ΔNF [dB]. – Ideal terms. \circ Single-frequency extractions. \times Approach (a)'s results. \triangle Approach (b)'s results.

band. The best results of the multi-frequency approaches concern the minimum noise figure and the optimum noise match, both in modulus and in phase. Notice that for some low frequencies (at which the device noise figure is also low, and therefore the percentage of states yielding unphysical measurements is high), the single-frequency approach fails completely, returning estimates of Γ_{opt} lying on the edge of the Smith Chart. On the contrary, the multi-frequency approaches show a significant immunity to these bad measurements, represented by the presence of a great number of other measurements.

The robustness of the multi-frequency algorithms was also tested against the pattern of source states. An example of extraction based on a 10-point pattern (magnitudes of 0.3 and 0.6, angles of $0^\circ, 72^\circ, \dots, 288^\circ$) is shown in Fig. 4. As expected, significantly larger errors are obtained in this case by the proposed multi-frequency algorithms in comparison to the 30-point pattern, but only for values of ΔNF above 0.5 dB.

In conclusion, although a more comprehensive study on the robustness of the proposed approaches to measurement errors is certainly desirable, we may already state that they outperform the plain reiteration of single-frequency extractions, even if followed by data fitting. Indeed, when measurement errors increase, the latter solution may become impractical, because single-frequency extractions may be so scattered that a clear pattern to be fitted cannot be identified

(see for instance the magnitude of the optimum noise match in Figs 3 and 4).

IV. EXPERIMENTAL RESULTS

In Section III a model was described which allows to describe the noise behavior of a high-frequency active device over a broad frequency range by means of 10 constant coefficients only. It was also anticipated that in some cases even simpler models are possible: in particular a good approximation can often be achieved neglecting coefficients β_2 and β_3 , since the imaginary part of \hat{c}_{12} is typically predominant on the real part and γ_3 , whose contribution does not typically play a significant role if not at high frequencies.

The 7-coefficient model thus obtained was used on devices from a well established, commercial GaAs technology, namely OMMIC ED02AH, featured by $0.18 \mu\text{m}$ gate length and both enhancement and depletion HEMTs. In order to obtain consistent data, two depletion-mode devices were measured with the same number of fingers (4×30 and $4 \times 50 \mu\text{m}$) and at the same bias point ($-0.1 \text{ V VGS}, 1 \text{ V VDS}$). Small-signal characterization of the devices was performed on wafer through a probe-tip SOLT calibration.

These devices were characterized by means of a Source-Pull test bench described in [9, 15]. The architecture of the test bench, as illustrated in Fig. 5, comprises two

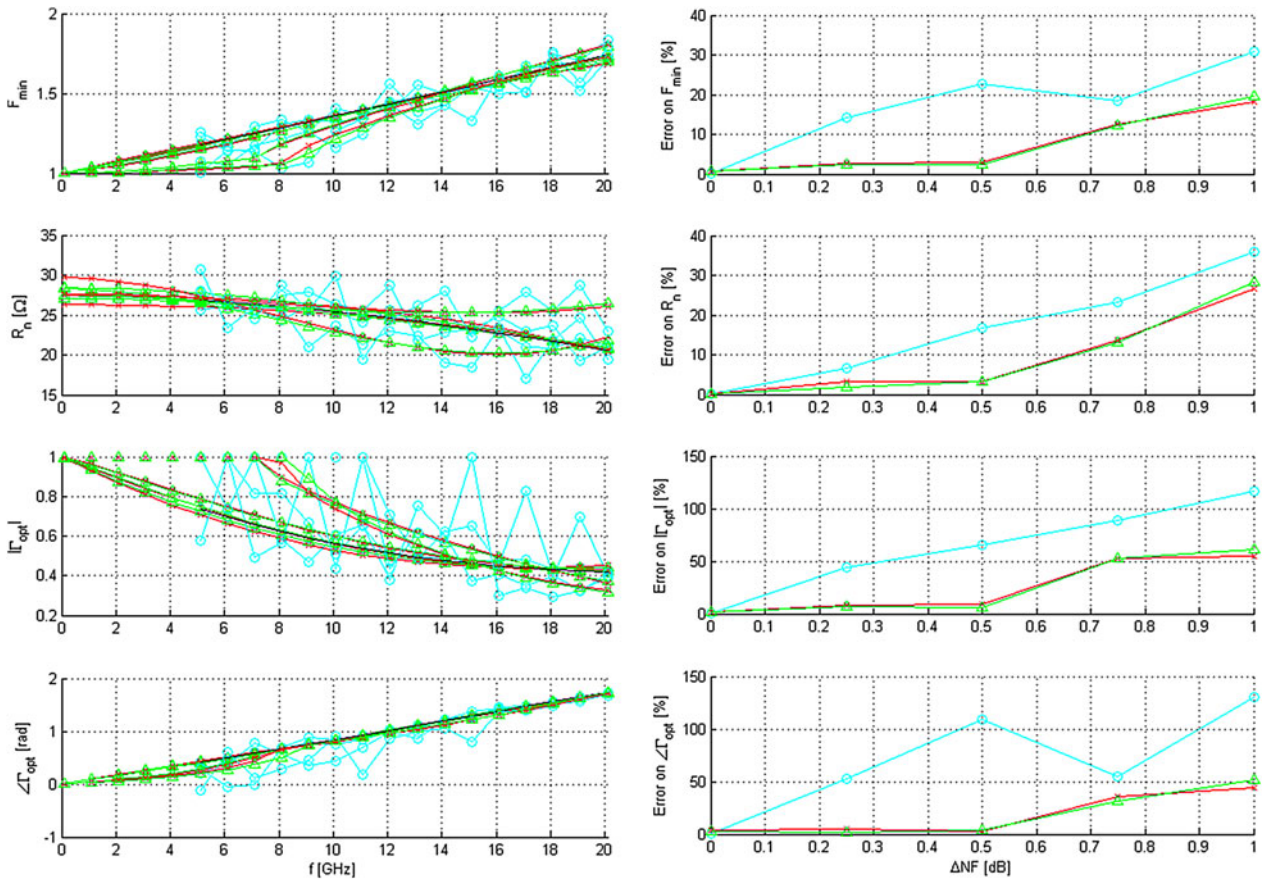


Fig. 4. Effect of measurement errors on noise parameter extraction for an ideal HEMT, with a 10-state pattern. Left side: example of extraction using the proposed methodologies for zero-mean measurement errors uniformly distributed in a range ΔNF [dB]. Right side: maximum percent errors versus ΔNF [dB]. – Ideal terms. \circ Single-frequency extractions. \times Approach (a)'s results. \triangle Approach (b)'s results.

electromechanical tuners and a complex RF switch matrix managing the signal paths during each measurement step. Although this bench is connectorized to operate up to 40 GHz (K connectors), it is currently limited in practice to about 20 GHz by the features of the input tuner (Focus Microwaves CCMT-1808) and of the receiver's low-noise pre-amplifiers. The authors are also working to improve accuracy by eliminating the VNA reference planes and adding other

reference planes at the external sections of the tuning blocks; moreover, the control routine of the output tuner is going to be refined, in order to guarantee better matching at the receiver's input section.

Extractions were performed on the 4×30 and $4 \times 50 \mu m$ HEMTs, setting a 61-point source pattern, made up of the origin of the Smith Chart, plus a double sweep on magnitude (0.15–0.75 by 0.15) and phase (30–360° by 30°). The results

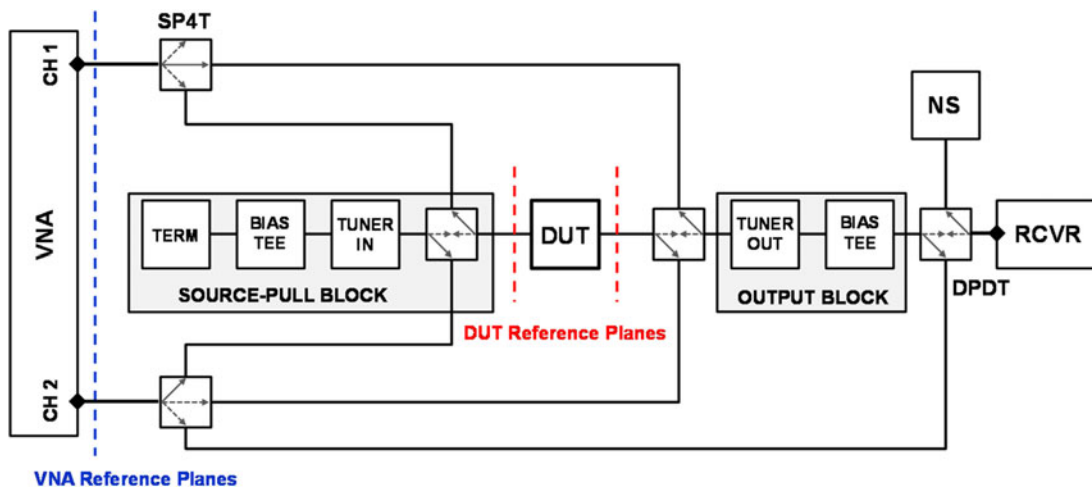


Fig. 5. Architecture of the Source-Pull test bench.

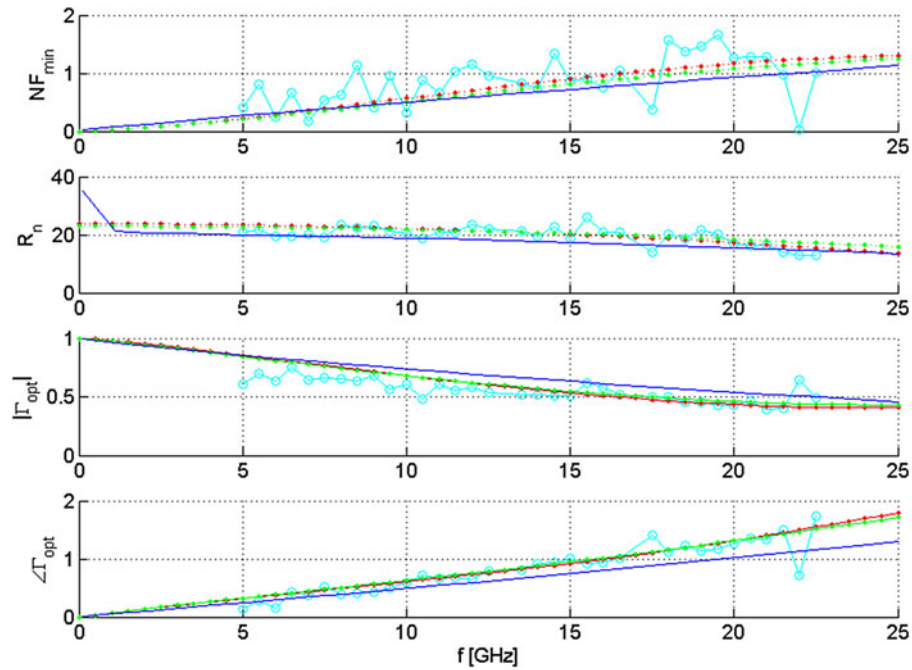


Fig. 6. Extracted noise parameters of the $4 \times 30 \mu\text{m}$ HEMT. — Reference model. \circ Single-frequency extractions. \times Approach (a)'s results. \triangle Approach (b)'s results.

are reported in Figs 6 and 7, respectively, in terms of NF_{min} [dB], R_n [Ω], $|\Gamma_{opt}|$, and $\angle\Gamma_{opt}$ [rad]. In these figures, again, the circle-marked traces represent the sequence of single-frequency, source-pull extractions, while “times” and “triangle” symbols indicate results of approaches (a) and (b) in Section III, respectively. Note that in this case real measurements are considered, so the “true” value of the parameters is not known: instead a continuous trace is plotted representing the same parameters extracted by a reference method

(based on the standard Pospieszalski model) by the foundry itself.

A good agreement is achieved between the proposed methods and the reference over the whole considered frequency range: in particular the minimum noise figures compare well, within 0.15 dB at 20 GHz, whereas the only non-negligible difference is on the phase of Γ_{opt} (17° at 20 GHz for both devices). However, since the proposed multi-frequency approaches are expected to predict the latter

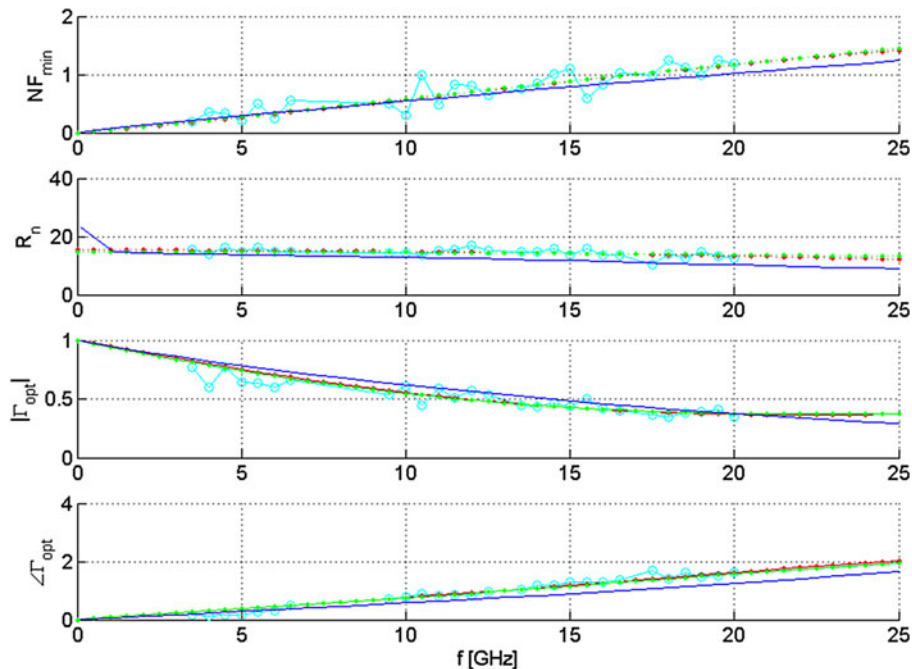


Fig. 7. Extracted noise parameters of the $4 \times 50 \mu\text{m}$ HEMT. — Reference model. \circ Single-frequency extractions. \times Approach (a)'s results. \triangle Approach (b)'s results.

parameter very accurately (see Section III), the authors are prone to attribute this discrepancy to an unaccounted-for change of the reference planes: indeed, the foundry model is extracted after fully de-embedding input and output access lines, while the other extractions are referred to the probe-tip planes – such hypothesis is corroborated by the fact that the same phase difference is found for both peripheries. Other minor deviations are easily explained by considering that the standard model is a scalable one, and therefore may not perfectly catch the individual features of each periphery, or device sample.

Finally, note how, as in the ideal case discussed in Section III, a direct extraction applied distinctly at each frequency results in irregular fluctuations of noise parameters, while the proposed approaches smooth such undesired behavior and allow obtaining a characterization quite in agreement with the reference model. This is achieved without the need for “exotic” mathematical functions to fit the behavior over frequency of the standard noise parameters.

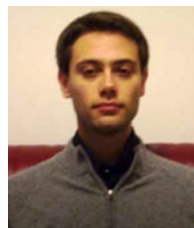
V. CONCLUSION

In this contribution an algorithm alternative to that proposed by Lane has been presented, allowing extracting the four noise parameters of a linear two-port from Single-Frequency, Source-Pull measurements through linear-system solving techniques. The novel method is mathematically equivalent to Lane's, but it takes advantage only of physical parameters and is suitable to be immediately extended to Multi-Frequency, Source-Pull extractions for high-frequency active devices. The validity of these approaches has been shown both in an ideal case and on real devices by comparison with a well established alternative methodology.

The presented extraction method does not need a previous knowledge of the FET equivalent circuit's topology, nor of the values of its elements, which is on the other hand a critical factor when the common noise temperature techniques are employed. This peculiarity, as well as the ease of software implementation, makes the proposed algorithm very well suited to quick characterization campaigns of active devices, thus avoiding the burden of a whole set of prior, heterogeneous, sometimes destructive measurements, together with the relevant extraction procedures, which are strongly dependent on the device and critical for the reliability of the results.

REFERENCES

- [1] Ciccognani, W.; Limiti, E.; Longhi, P.E.; Renvoise, M.: LNAs for radioastronomy applications using advanced industrial 70 nm metamorphic technology. *IEEE J.Solid-State Circuits*, **JSSC-45** (10) (2010), 2008–2015.
- [2] Pucel, R.A.; Haus, H.A.; Statz, J.: Signal and noise properties of Gallium Arsenide microwave field-effect transistors. *Adv. Electron. Electron Phys.*, **38** (1975), 195–265.
- [3] Gupta, M.S.; Greiling, P.T.: Microwave noise characterization of GaAs MESFET's: determination of extrinsic noise parameters. *IEEE Trans. Microw. Theory Tech.*, **36** (4) (1988), 745–751.
- [4] Pospieszalski, M.W.: Modeling of noise parameters of MESFETs and MODFETs and their frequency and temperature dependence. *IEEE Trans. Microw. Theory Tech.*, **37** (9) (1989), 1340–1350.
- [5] Tasker, P.J.; Reinert, W.; Braunstein, J.; Schlechtweg, M.: Direct extraction of all four transistor noise parameters from a single noise figure measurement, in *Proc. 22nd European Microwave Conf.*, 5–9 September 1992, 157–162.
- [6] Dambrine, G.; Cappy, A.; Delos, E.: A new method for on-wafer high frequency noise measurement of FETs, in *Proc. IEEE MTT-S Int. Microwave Symp. Digest*, 10–14 July 1991, 169–172.
- [7] De Dominicis, M.; Giannini, F.; Limiti, E.; Serino, A.: Direct noise characterization of microwave FET using 50 Ω noise figure and Y-parameter measurements. *Microw. Opt. Technol. Lett.*, **44** (6) (2005), 565–569.
- [8] Ciccognani, W. et al.: Extraction of microwave FET noise parameters using frequency- dependent equivalent noise temperatures, in *Proc. Int. Microwave and Optoelectronics Conf. (IMOC)*, Salvador (Brasile), 29 October–1 November 2007, 856–860.
- [9] Bentini, A.; Ciccognani, W.; Colangeli, S.; Scucchia, L.; Limiti, E.: Highly reliable characterization approaches oriented to active device noise modeling, in *Proc. Int. Symp. on Microwave and Optical Technology (ISMOT 2011)*, Prague (Czech Republic), 20–23 June 2011.
- [10] Lane, R.Q.: The determination of device noise parameters. *Proc. IEEE*, **57** (8) (1969), 1461–1462.
- [11] Engberg, J.; Larsen, T.: *Noise Theory of Linear and Nonlinear Circuits*. John Wiley & Sons Ltd., Chichester, England, 1995.
- [12] Boudiaf, A.; Laporte, M.: An accurate and repeatable technique for noise parameter measurements. *IEEE Trans. Instrum. Meas.*, **42** (2) (1993), 532–537.
- [13] De Dominicis, M.; Giannini, F.; Limiti, E.; Saggio, G.: A novel impedance pattern for fast noise measurements. *IEEE Trans. Instrum. Meas.*, **IM-51** (3) (2002), 560–564.
- [14] Reveyrand, T. et al.: GaN transistor characterization and modeling activities performed within the frame of the KorriGaN project. *Int. J. Microw. Wirel. Technol.*, **2** (01) (2010), 51–61.
- [15] Pantellini, A. et al.: GaN-on-silicon evaluation for high-power MMIC applications, in *Proc. workshop on advanced semiconductor materials and devices for power electronics applications (HeteroSiC-WASMPE 2011)*, Tours (France), 27–30 June 2011.



Sergio Colangeli was born in Roma, Italy, in 1984. He received a degree in Electronic Engineering in 2008 from the University of Roma Tor Vergata, where he has recently finished a Ph.D. course in Telecommunications and Microelectronics. His main research activities are in the field of low-noise design methodologies for microwave

applications, and he is also involved in collaborations with high-tech companies, both Italian and foreign ones, as a designer. More recently, he has been working on the realization of an automated, general-purpose test-bench, especially suited to source-pull noise measurements. To enhance the capabilities of this test-bench (and possibly similar ones), he is now engaged in the development of extraction algorithms to apply to source-pull noise data.



Walter Ciccognani was born in Roma, Italy, in 1977. He received an electronic engineering degree in 2002 and a Ph.D. degree in 2007 from the University of Roma Tor Vergata, and he is currently working in collaboration with that University. His main research activities are in the field of linear microwave circuit design methodologies, linear and noise

analysis/measurement techniques, and small-signal and noise modeling of microwave active devices. He has a long experience as a HMIC and MMIC designer, having also frequently collaborated with national and foreign high-tech corporations.



Mirko Palomba was born in Marino, Italy, in 1984. He received a degree in Electronic Engineering in 2010 from the University of Roma Tor Vergata, and he is currently a Ph.D. student at the same university. He is mainly interested in the research field of signal conditioning schemes in microwave electronics circuits, however his activities cover other topics, such as: noise and power amplifiers, core-chips, frequency converters, filters, distributed

amplifiers. He has been working as a HMIC and MMIC designer, and as such has collaborated with national and foreign high-tech corporations.



Ernesto Limiti has been a full professor of electronics in the engineering faculty of the University of Roma Tor Vergata since 2002. His research activity, which has produced more than 200 publications on referred international journals and presentations at international conferences, is focused on three main lines in the area of microwaves and millimeter-waves, namely, characterization and modeling of active and passive devices, design methodologies of nonlinear circuits, and development of extremely low-noise amplifiers and receiving subsystems.

Prof. Limiti acts as a referee or editorial board member of international journals of the microwave and millimeter-wave electronics field and he is in the steering committee of several international conferences and workshops. He is actively involved in research activities with many European and Italian research groups, and he is in tight collaboration with high-tech Italian (SELEX-ES, Thales Alenia Space, Rheinmetall, Elettronica S.p.A., Space Engineering, etc.) and foreign (OMMIC, Siemens, UMS, etc.) companies.

Published online by Cambridge University Press